RSC Advances

The Improvement of Hemostatic and Wound Healing Property of

Chitosan by Halloysite Nanotubes

Mingxian Liu[a,1], *Yan Shen*[b,1], *Peng Ao*[a], *Libing Dai*[b], *Zhihe Liu*[b], *Changren Zhou*[a,*]

[a]Department of Materials Science and Engineering, Jinan University, Guangzhou 510632, China.

[b]Guangzhou Institute of Traumatic Surgery, Guangzhou Red Cross Hospital Medical College, Jinan

University, Guangzhou 510220, China.

[1] The authors contributed equally to this work.

* Corresponding author: tcrz9@jnu.edu.cn

Abstract

As tube-like natural nanomaterials, halloysite nanotubes (HNTs) have potential applications in wound healing due to their high mechanical strength, good biocompatibility, hemostatic property, and wound healing ability. Here, we have developed flexible 3D porous chitosan composite sponges via the addition of HNTs. Morphological observation, mechanical property, porosity, swelling ability, and degradation behavior in phosphate buffer of the chitosan-HNTs composite sponges were investigated by various physico-chemical methods. Compared to pure chitosan sponge, the composite sponges exhibit a similar porous morphology but maximum 8.8-fold increased compression mechanical properties. The elastic modulus, compressive strength, and toughness of the composite sponges increase by HNTs simultaneously. The whole blood clotting experiment suggests that HNTs can increase the blood clotting rates of chitosan. The composite sponges with 67% HNTs shows 89.0% increase in the clotting ability compared with pure chitosan. Cytocompatibility of the composite sponges is confirmed by cell attachment and infiltration of fibroblast and vascular endothelial cells. *In vivo* evaluation on full-thickness excision wounds in experimental Sprague−Dawley rats reveal that these composite sponges enhance the wound healing property especially at early stage. The composite sponges show 3.4~21 fold increased wound closure ratio compared with that of pure chitosan after one week. The addition of HNTs helps for faster re-epithelialization and collagen deposition. All these data demonstrate the potential applications of the chitosan-HNTs composite sponges for burn wounds, chronic wounds, and diabetic foot ulcers.

Keywords: cell spreading, mechanical properties, haemostasis, microstructure, wound healing

1. Introduction

As the largest organ in area of human body, skin is the first outside barrier between body and environment. Skin performs many functions such as protection, sensation, control of evaporation, storage and synthesis, absorption, and water resistance. However, the trauma or other injuries always lead to varying degrees of damage and skin defects. Skin generally needs to be covered with a dressing immediately after it is damaged . The wound healing can proceed through regeneration and reconstruction by a series of pathophysiological processes which involves the complex interactions among the different types of skin cells, cytokines and extracellular matrix . For the wound healing goal, many types of dressing materials have been explored such as hydrogel [1, 2], membrane [3, 4], sponge [5], non-woven fabrics and nanofibers [6, 7]. Sponges are soft and flexible materials with well interconnected microporous structure that show many unique characteristics such as good fluid absorption capability, cell interaction and hydrophilicity. But they have some serious flaws such as low hemostasis ability, poor mechanical property, limited healing ability, and high fabrication cost, restricting their practical applications. Many synthetic or natural macromolecules have been selected as the matrices for wound dressing to improve the healing process [8]. Among these macromolecules, chitosan, derived from natural resources and available abundantly, is considered as a promising material for tissue regeneration [9]. The features of chitosan for using in wound healing include biocompatibility, biodegradability, hemostatic activity, anti-inflectional activity and with property to accelerate wound healing [4, 10]. Furthermore, chitosan can easily be processed into membranes, gels,

nanofibers, beads, nanoparticles, scaffolds, and sponges for wound dressing applications. Chitosan has the functions in the acceleration of infiltration of polymorphonuclear cells at the early stage of wound healing, followed by the production of collagen by fibroblasts [11]. However, the hemostatic performance, healing ability, and flexibility of chitosan should be further improved in order to expand its applications as wound dressing materials.

Clays are important adjutants and supports for medical products, since they have many physicochemical, mechanical, and biological properties such as high absorption ability, drug loaded ability, absence of toxicity, indifference to other raw materials, and complex formation properties [12, 13]. Among various types of clays, one-dimensional halloysite nanotubes (HNTs) have been used to improve the mechanical properties, drug loading properties, cell attachment and hemostatic performance of polymers in the recent years [14]. HNTs are natural inorganic nanomaterials, with a chemical formula of $Al_2Si_2O_5(OH)_4 \cdot nH_2O$. The length of HNTs is in the range of 0.2–1.5 μm, while the inner diameter and the outer diameter of tubes are in the ranges of 10–40 nm and 40–70 nm, respectively. The aspect ratio (L/D) of HNTs is in the range of 10-50. The empty lumen microstructures and porosity of HNTs enable them a high loading and absorption ability for active compounds [14]. Therefore, HNTs are usually used in drug delivery systems and waste water treatment [15, 16]. Recent researches have suggested that HNTs are cytocompatible and can potentially be used as tissue engineering scaffold materials [17, 18]. These unique properties of HNTs inspire us to explore their application in wound healing. Interestingly, in traditional Chinese medicine, halloysite (with a Chinese traditional medicine name "Chishizhi") was commonly used as wound dressing materials in the form of powder. And they have been confirmed with the efficacy of hemostasis and wound healing. However, up to now there is no scientific report on the wound

healing applications of HNTs. In contrast, there are numerous papers and patents on other clay

minerals for using as wound dressing materials [19-21].

Chitosan porous scaffolds prepared by lyophilization or electrospinning sever as good candidate for

the wound treatment with benefits of capability of drug/growth factors delivery[22-25]. These active

compounds can significantly accelerate the wound healing process. However, the preparation process

of drug-loaded chitosan scaffolds is complicate. Also, the loaded growth factors are easily degraded

by proteinases or removed by exudate before reaching the wound bed[22]. Therefore, preparing high

healing performance chitosan dressing materials without drugs is still challenge.

In the present work, the chitosan-HNTs composite sponges with different HNTs loadings were

prepared by lyophilization method. The influences of HNTs on the physicochemical, microstructure,

cytocompatibiity, *in vivo* wound healing ability of chitosan sponge were investigated. HNTs improve

the mechanical properties, cell attachments, hemostatic performance, and wound healing rate of

chitosan simultaneously. The composites sponges have maximum 8.8-fold increased compression

strength, 89.0% increased clotting ability, and 21-fold increased wound closure ratio compared with

pure chitosan sponges. Also, the composite sponges have controllable porosity, swelling ratio, and

degradation properties by changing of HNTs contents. In addition, the cost of the composite sponges

is much lower than the pure chitosan sponges, facilitating their commercialization. This works open a

new area of HNTs' biomedical applications and provide a novel routine for the high performance

wound dressing materials by simple fabrication method and with low cost.

2. Experimental

2.1 Raw materials

Chitosan was purchased from Jinan Haidebei Marine Bioengineering Co. Ltd (China). Its deacetylation and viscosity-average molecular weight was 95% and 600,000 g/mol, respectively. Raw halloysite was mined from Hunan province (China) and purified before using. The elemental composition of purified HNTs by X-ray fluorescence (XRF) was as follows (wt.-%): SiO_2, 54.29; Al_2O_3, 44.51; Fe_2O_3, 0.63; TiO_2, 0.006. The Brunauer–Emmett–Teller (BET) surface area of the used HNTs was 50.4 m^2/g. All other chemicals used in this work were analytical grade. Ultrapure water from Milli-Q water system was used for preparing the aqueous solutions.

2.2 Preparation of the chitosan-HNTs composite sponge

The chitosan-HNTs composite sponges were prepared by solution mixing and subsequently freeze-drying method. The raw chitosan was first treated with acetic acid (2% concentration) under stirring with 10 hours. The insoluble fraction was separated by centrifugation at 8000 rpm for 15 min and the supernatant containing the chitosan was isolated. The purified chitosan was obtained by freeze-drying. The typical procedure for preparing the composite sponges was described below and depicted in Figure 1. 2 g of chitosan was dissolved in 100 ml of 2 wt.-% acetic acid solution under mechanical stirring. Then the calculated amount of HNTs powder was added into the chitosan solution. The mixture solution was continuously stirred overnight under ambient temperature and then treated by ultrasonic for 30 min to obtain a good dispersion of HNTs and the interfacial adsorptions. Then the solutions were poured into cylinder plastic mold. Subsequently, they were frozen into ice at -20°C overnight in a refrigerator and then lyophilized at -80°C using Christ freeze dryer ALPHA 1-2/LD plus. Then the scaffolds were immersed for 2 h in 2% NaOH for neutralizing

6

the residual acetic acid and extensively rinsed in sterile distilled water. Finally the scaffolds were freeze dried and stored for further use. For comparison, pure chitosan sponge was also prepared in the same way but without addition of HNTs. The sample codes of the composite sponge (CS2N1, CS1N1, CS1N2, CS1N4) represented the weight ratio of chitosan (CS) and HNTs (N). For example, in CS1N2 sample the weight ratio of chitosan and HNTs was 1:2.

Figure 1 Schematic representation of the preparation of chitosan-HNTs composite sponges.

2.3 Physicochemical characterization of the chitosan-HNTs composite sponge

Scanning electron microscopy (SEM) Before SEM observation, the sponges were sectioned and were sputter coated with 10 nm thick gold–palladium layer using a sputter coater (BALTEC SCD 005). The morphology of the sponges was observed with a Philips XL30 ESEM and Hitachi S-4800 FE-SEM (for high magnification photos).

Porosity. The porosity of the sponges was determined using the reported method [26]. First, the sponges were immersed in absolute ethanol until it was saturated. Afterwards, the sponges were weighed before and after the immersion in alcohol. The porosity was calculated using the formula,

$$porosity~(\%) = \frac{W_2 - W_1}{\rho V_1} \times \%$$

Here, W_1 and W_2 was the weight of sponges before and after immersion in alcohol, respectively. V_1 is the volume before immersion in alcohol; ρ is a constant (the density of alcohol). All samples were triplicated in the experiment.

Swelling ratio. The equal volume sponges were immersed in phosphate buffered saline (PBS) (pH 7.4,

7

37°C). The sponges were taken out at predetermined time intervals and water that adhered on the surface was removed by gently blotting with filter paper and immediately weighed (W_d). The swelling ratio was calculated by the following formula,

$$DS\,(\%) = \frac{W_w - W_d}{W_w} \times 100\%$$

Here, DS was the degree of swelling; W_w and W_d represented the wet and dry weight of the sponges respectively.

In vitro **biodegradation behavior.** The sponge samples were equally weighed and immersed in lysozyme (10000 U/mL) containing the medium and incubated at 37°C for 28 days. The samples were removed after 7, 14, 21 and 28 days from the medium containing lysozyme and washed with deionized water to remove ions adsorbed on surface and freeze-dried. The dry weight was noted as W_t and initial weight as W_i. The degradation of the sponges was calculated using the formula,

$$degradation\,(\%) = \frac{W_i - W_t}{W_i} \times \%$$

Compression property. The compression property of pure chitosan and the chitosan-HNTs composite sponges was determined using Universal Testing Machine (Zwick/Roell Z005, Germany) under 25°C according to ASTM D5024-95a. The samples for the test were cylinder samples with diameter of ~16 mm and thickness of ~14 mm. The crosshead speed was 2 mm/min, and up to 85% reduction in specimen height. The stress-strain curves for every sample were recorded automatically by the testXpert® II V2.0 software. Compressive modulus was calculated as the slop of the initial linear portion of the stress-strain curves. The deformation recovery ratio (R) was calculated by the following equation,

$$R\,(\%) = \frac{h_f - (1 - \varepsilon)h_0}{\varepsilon h_0} \times \%$$

Here, h_f was the final height of sample after 30 min of the compressive testing; h_0 was the initial height

of the samples before compressive testing; ε was the deformation ratio when stopping the

compression test (ε=85% for the present work). Five samples were used to obtain reliable data.

2.4 Cell cultures on the chitosan-HNTs composite sponges

Fibroblasts were isolated from a human skin biopsy and used at passage 3~4. Endothelial cells were

from dermal microvascular origin, and keratinocyte cultures were established from human skin

biopsies.

The sterile pure chitosan and chitosan-HNTs sponges were seeded with NIH 3T3 and vascular

endothelial cells in a 24-well plate at a concentration of 1×10^5 cells/well. After 3 days of incubation,

the sponges were washed with PBS and fixed with 2.5% glutaraldehyde for 1 h. The samples were

thoroughly washed with PBS and sequentially dehydrated through a series of graded-ethanol

solutions, freezing-dried, gold sputtered in vacuum and observed by SEM.

2.5 Whole-blood clotting and platelet activation evaluation of chitosan-HNTs composite sponges

The blood clotting study of the materials was done according to the literatures [24, 26]. Blood was

drawn from human ulnar vein using BD Discardit II sterile syringe and mixed with anticoagulant

agent acid citrate dextrose at the ratio of 85%:15%. Triplicate samples were used for this study and

blood without materials was used as negative control. Blood was added to 10 mg sponges and

freeze-dried HNTs powder (from 5 wt.% HNTs aqueous dispersion) which were placed in 6-well plate,

which was followed by the addition of 10 µL of 0.2 M $CaCl_2$ solutions to initiate blood clotting. These

sponges then were incubated at 37 °C for 10 min. Fifteen milliliters (15 mL) of distilled water was then

added dropwise without disturbing the clot. Subsequently, 10 mL of solution was taken from the

dishes and was centrifuged at 1000 rpm for 1 min. The supernatant was collected for each sample and

kept at 37°C for 1 hour. Two hundred microliters (200 μL) of this solution was transferred to a 96-well plate. The optical density was measured at 540 nm using a plate reader (Multiskan MK3, Thermo Electron Corporation).

Platelet activation study was conducted as follows. Platelet-rich plasma (PRP) was isolated from the blood by centrifugation of blood at 2500 rpm for 5 min. One hundred microliters (100 μL) of PRP was poured onto the sponge piece (10 mg) and incubated at 37°C for 20 min. The sponges were then washed three times with PBS solution and fixed using 0.1% glutaraldehyde solution. The sponges were dried and then SEM images were taken.

2.6 *In vivo* evaluation of wound healing properties of chitosan-HNTs composite sponges

All experimental procedures were performed according to the Guide for the Care and Use of Laboratory Animals and were in compliance with the guidelines specified by the Chinese Heart Association policy on research animal use and the Public Health Service policy on the use of laboratory animals. Sprague−Dawley (SD) rats, weighing 200−250 g and 4−6 weeks of age, were used in this study. The rats were divided into seven groups and each group contains three rats (n=3); rats were allowed to take normal rat feed and water without restriction. On the day of wounding, the rats were anaesthetized by intramuscular injection of 35.0 mg/kg ketamine and 5.0 mg/kg xylazine. The dorsal area of the rats depilated and the operative area of skin cleaned with alcohol. Full thickness wounds (1.5 cm×1.5 cm) were prepared by excising the dorsum of the rat using surgical scissors and forceps. The prepared wounds were then covered with the pure chitosan sponge, chitosan-HNTs composites sponge, commercially available adhesive wound dressing (AWD), and oily cotton gauze (OY). After applying the dressing materials, the rats were housed individually in cages under room temperature.

The dressing materials were changed at week 1, 2, and 3. During the changing of dressings, photographs were taken and the wound area was measured using a soft plastic sheet. The sheet was kept on top of the wound and area was marked using a marker pen. The marked area was then transferred to graph sheet for getting the exact value. After Week 4, the skin wound tissue of the rat was excised, fixed with 10% formalin, and stained with a hematoxylin−eosin (H&E) reagent for histological observations. The amount and the type of collagen deposition were determined by Masson and Sirius Red (SR) staining, respectively.

3. Results and Discussion

3.1 SEM observation of construction of the chitosan-HNTs composite sponges.

The morphology of the lyophilized chitosan and chitosan-HNTs sponges was investigated by SEM (Figure 2). All the sponges show honeycomb-like porous microstructures with a pore diameter of about 200 μm and pore-wall thickness in scores of nanometers. The addition of HNTs has slight effect on the pore structure of the chitosan sponge even with 80 wt.-% loading. Such interconnected micro-pore structures of the sponges provide efficient channels for rapid liquid gas transport, benefiting to their wound healing applications. In the enlarge images of the composite sponges (Figure 2f), it is clear that HNTs are embedded in chitosan matrix with indistinct interfaces, suggesting their strong interfacial interactions between HNTs and chitosan due to their hydrogen bonding and electrostatic attraction [27]. It should be noted that the roughness of the pore-wall for the sponges may be increased by the presence of the nanoparticles [27-29]. And the roughness surface benefit the adhesion and growth of cells compared with smooth surface [29, 30]. This is also confirmed in this work and will show in the cell experiment result below.
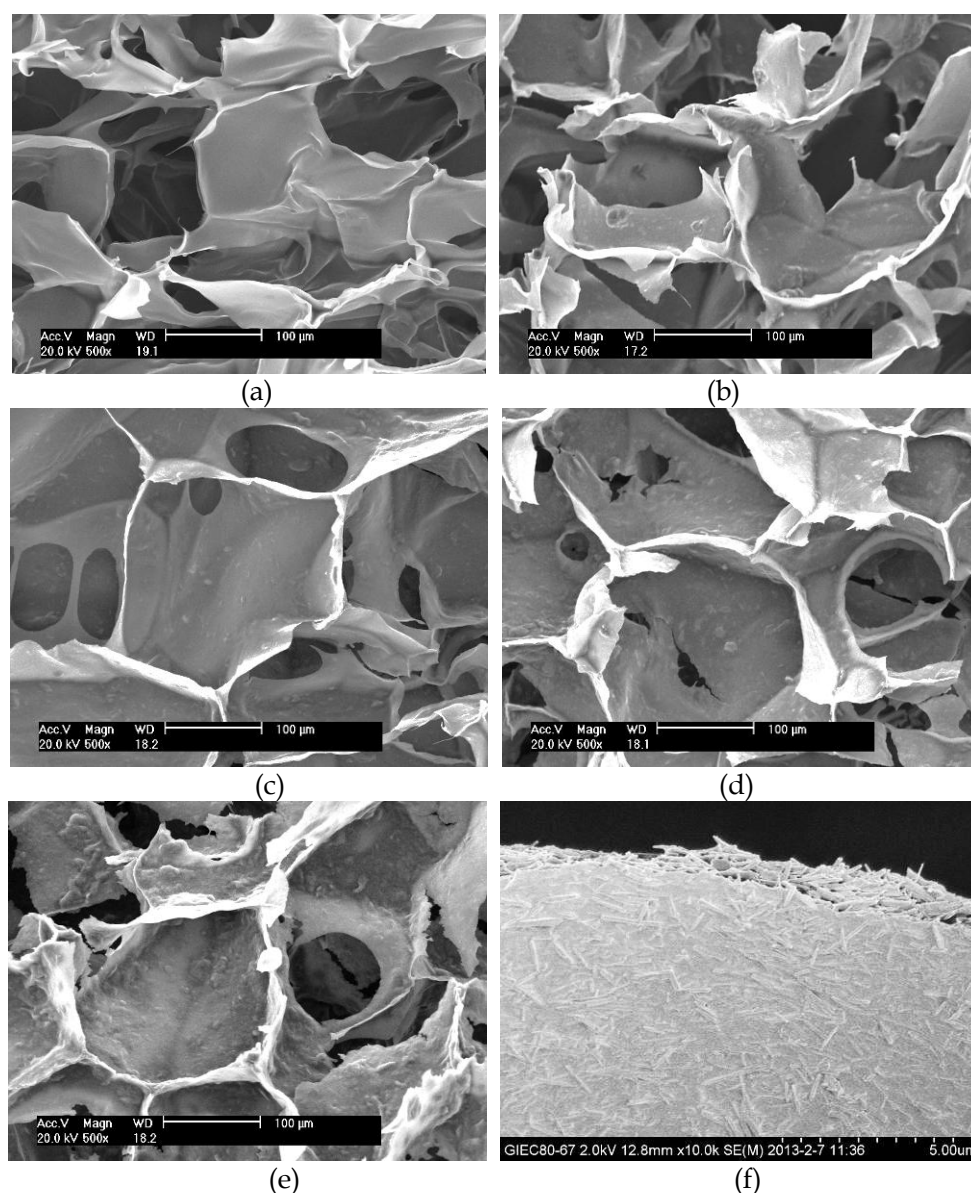
Figure 2 SEM images of pure chitosan (a), CS2N1 (b), CS1N1 (c), CS1N2 (d), CS1N4 (e) and amplifying region in (c) which showing the presence of HNTs (f).

3.2 Physicochemical characterization of chitosan-HNTs composite sponges.

The density and porosity of the prepared sponges were determined and the results are shown in Figure 3(a). As expected, the density of the chitosan-HNTs sponges is linearly increased with the loading of HNTs. This is attributed to fact that the concentration of chitosan solutions is fixed but with the gradual addition of HNTs into the aqueous solution when preparing the sponges. That is to say, in the same volume of the sponges, the materials amount in the composite sponges increase with the

loading of HNTs. As a result, the density of the composite sponges increases by the addition of HNTs. The increased density of the sponges is beneficial to the improvement of the mechanical properties such as dimensional stability. A slight decrease in porosity of the sponges is obtained with the increase in HNTs loadings. The pure chitosan sponges have the maximum porosity of 94.3%, while the porosity is decreased to 80.7% for the CS1N4 sponge. The porosity of the sponges is a critical factor determining the gas permeability, fluid absorption capability, cell migration behavior, and mechanical performance. The high porosity of pure chitosan sponges is helpful for absorbing exudate from the wound surface and facilitate the transfer of the nutrients and medium for the cells. However, the sponges with high porosity suffer from the weak stress resistant especially during compression. The influence of the porosity on the mechanical performance of the sponges will be discussed in the following section.

The comparison of the swelling ratio of the pure chitosan and chitosan-HNTs sponges in PBS solutions is given in Figure 3(b). At the day 1, the sponges have the swelling ratios in the range of 8.8~16.4. With the extension of immersing time, all the samples exhibit an increasing trend for the swelling ratio. For example, the swelling ratio of CS1N1 sponges increases from 14.7 at day 1 to 17.2 at day 7. With respect to difference of the swelling ratio among the samples, apart from pure chitosan's, the swelling ratios of the composite sponges decrease with HNTs loadings. The hydrophilicity of the materials and the pore structure of sponge affect their swelling ratios. The decreased degree of swelling is attributed to the lowered porosity as shown in Figure 3(a) and the relatively low water absorption ability of HNTs (3~5.3%) [31] compared with the same quality of chitosan (~48%) [32] in the composite sponges. The pure chitosan sponge has a moderate swelling ratio among the samples, indicating that the water retention of the sponges can be adjusted by the addition of HNTs. The

hydrophilicity of the prepared sponges is expected to accelerate the blood coagulation process and enhance cell attachment and proliferation during the tissue regeneration process.

The structural integrity of the sponges under biologically relevant pH and ion concentrations is vital to ensure sufficient maintenance of mechanical strength and porosity for cell interactions. The weight losses of the pure chitosan and chitosan-HNTs composite sponges were monitored as a measure of degradation in biological buffer (PBS) over 28 days (Figure 3c). It can be seen that with the increase in the contact time, all the samples decrease the weight in the PBS. With incorporation of the HNTs, chitosan sponges show a decreased weight loss ratio. This is attributed to the primary degradation of the sample is related to the chitosan chain breakage while HNTs nearly do not degrade in the PBS solutions. With the increase of the HNTs loading, the relative contents of the chitosan in the samples decrease. As a result, the weight loss ratio of the composites is lower than that for pure chitosan. Furthermore, the interfacial interactions between HNTs and chitosan can constrain the molecular mobility of chitosan. And HNTs play the role of protector of chitosan against the attack of the medium. However, when the loading of HNTs is increased to 80 wt.% (CS1N4), the weakened interfacial interactions may increase the expose chance for the chitosan chain in the medium. As a result, the CS1N4 shows a slight increasing in the weight loss ratio compared with that of CS1N2. The decreased degradation rate of chitosan by the nanofillers has also been reported [26, 33, 34].

(a)

(b)

(c)
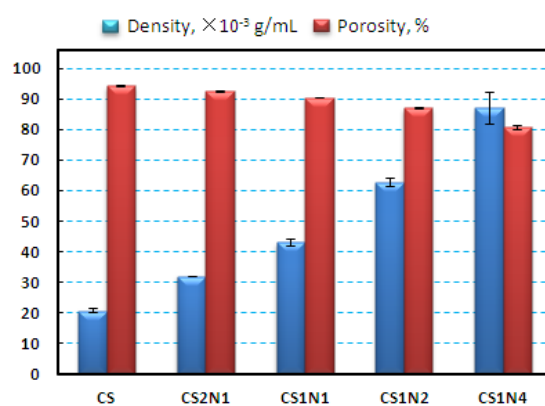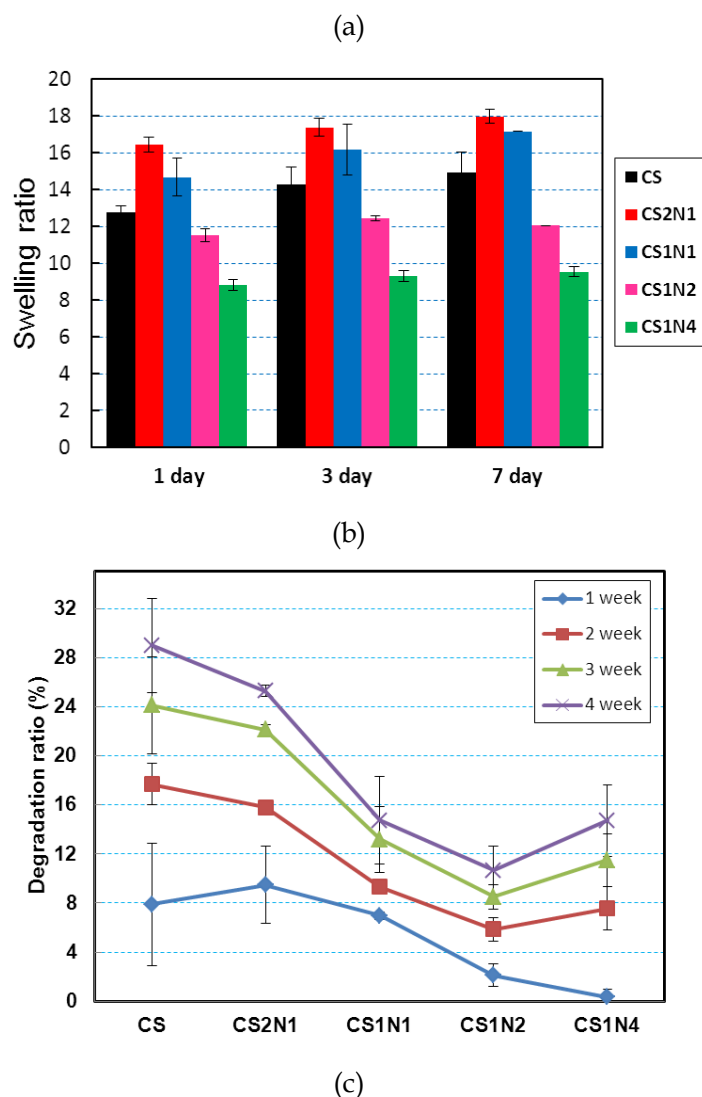
Figure 3 Density/porosity (a), swelling ratios in PBS at 37°C (b) and degradation ratio (c) of the pure chitosan and chitosan-HNTs composite sponge.

3.3 Mechanical property of chitosan-HNTs composite sponges.

The influences of HNTs on the mechanical properties of chitosan sponges were investigated via the compression test. Figure 4 shows typical compressive stress-strain curves for pure chitosan and chitosan-HNTs composite sponges. Table 1 summarizes the mechanical properties data of the samples. HNTs can effectively increase the compressive modulus and strength of chitosan; and the increasing trend is proportional with the HNTs loadings. For example, the elastic modulus of CS1N4 is 3054 kPa, which is 8.8-fold relative to that of pure chitosan. The reinforcing ability of HNTs for chitosan is attributed both the high strength of the tubes and the good interfacial interactions in the composite

15

systems as illustrated before [17, 27]. Additionally, the decreased porosity by the incorporation of HNTs also helps for the increase in the compression properties. On the other hand, the flexibleness is critical for the practical application of wound dressing materials as well as their compression strength [35]. A material with proper flexibleness is benefit for their closely contact on the wound surface. Due to the difficulty for direct determining the impact toughness of the sponges, we employed the deformation recovery ratio to compare their flexibleness. From Table 1, all the composite sponges exhibit higher deformation recovery ratio compared with pure chitosan. The maximum deformation recovery ratio of the composite sponges (CS1N1) is 3-fold compared to pure chitosan, suggesting the good elasticity of the samples. The lowered deformation recovery ratio of the composite sponge at relatively high HNTs loading (CS1N2 and CS1N4) is attributed to both the decrease of the chitosan content and the weakened interfacial interactions. All the results demonstrate that the chitosan-HNTs composite sponges can fulfill the essential requirements for dressing materials to use on wound healing under high stresses and can provide mechanical support for protection of wound surfaces and facilitation of cells attachment.
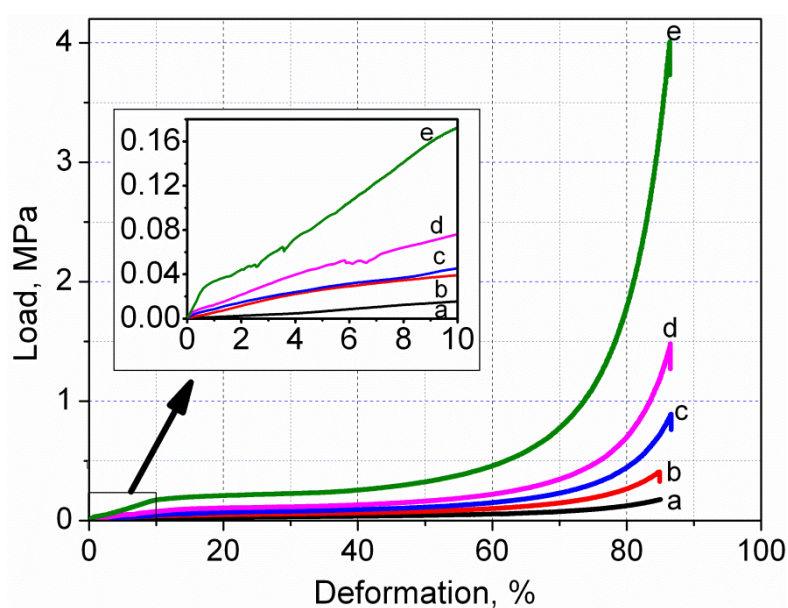
Figure 4 Compressive stress-strain curves for chitosan-HNTs composite sponges: (a)CS; (b)CS2N1; (c)CS1N1;

(d)CS1N2; (e)CS1N4. The inset shows the region for determining compressive modulus of the samples.

Table 1 Summary of the mechanical properties data (Data in the parentheses indicates the standard deviations).

Sample	Elastic modulus (kPa)	Stress at 60% strain (kPa)	Maximum load (N)	Deformation recovery ratio (%)
CS	311.7 (259.0)	55.1 (5.7)	59.9 (20.9)	9.36 (6.98)
CS2N1	408.7 (239.2)	101.0 (3.1)	75.2 (9.9)	23.11 (3.72)
CS1N1	578.3 (456.1)	151.0 (15.6)	122.0 (47.5)	30.91 (4.14)
CS1N2	1428.8 (860.2)	220.0 (10.8)	260.8 (76.2)	19.33 (4.89)
CS1N4	3054.0 (1115.5)	458.0 (24.8)	870.4 (523.6)	9.85 (5.39)

3.4 Evaluation of whole-blood clotting and platelet activation.

In order to evaluate the influence of HNTs on the blood clotting behavior of chitosan sponges, whole blood was contacted with the prepared sponges. For comparison, the freeze-dried HNTs powder was selected as control. The appearance of the blood clotting caused by the sponges and HNTs powder is shown in Figure 5. It can be seen that the chitosan-HNTs composite sponges have much higher blood clotting ability in comparison with pure chitosan or neat HNTs. When dipping the blood on the composite sponges, the blood can be rapidly absorbed in the porous composite sponges. But for the pure chitosan sponges and HNTs powder, the blood seem hardly infiltrate the materials. To quantify comparison the clotting ability of the samples, the red blood cells (RBCs) that are not trapped in the sponges and the HNTs were hemolyzed with water, and the absorbance of the resulting hemoglobin solution was measured (Figure 6). A higher absorbance value of the hemoglobin solution thus indicates a slower clotting performance. All the composite sponges exhibit lowered absorbance than the pure chitosan sponge. For example, the CS2N1 and CS1N2 sponge shows 82.2% and 89.0% decrease in the absorbance value respectively compared with pure chitosan, suggesting its high clotting ability. In a similar research, adding nano ZnO, however, has nearly no effect on the clotting properties of chitosan and β-chitin[26, 36]. Incorporation of nano chondroitin sulfate into chitosan–hyaluronan blend can lead to ~50% decrease in the absorbance value of the hemoglobin

17

solution[37]. Therefore, HNTs are superior to other nanoparticles in the view of the clotting ability.

(a)

(b)

(c)

(d)
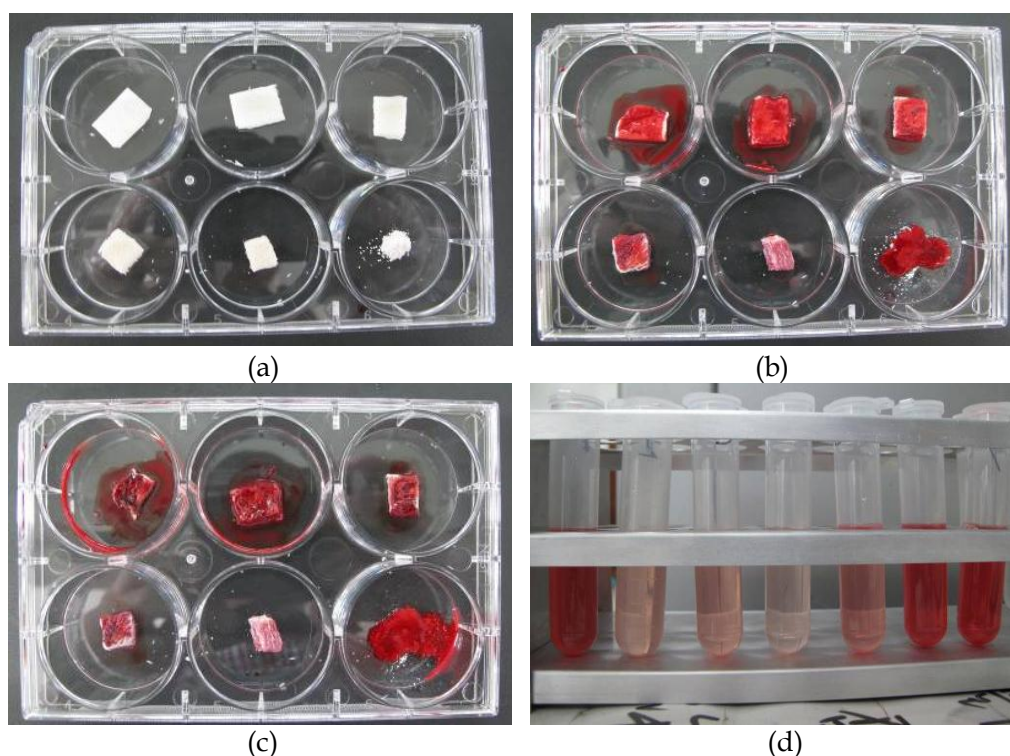
Figure 5 Photographs of the sponges and freeze-dried HNTs powder (a), blood on the materials with $CaCl_2$ solution (b), clotted blood on the materials after culture at 37°C for 30 min (c), and the corresponding aqueous solution (d). From left to right and from top to bottom: CS; CS2N1; CS1N1; CS1N2; CS1N4, HNTs powders, and blood.
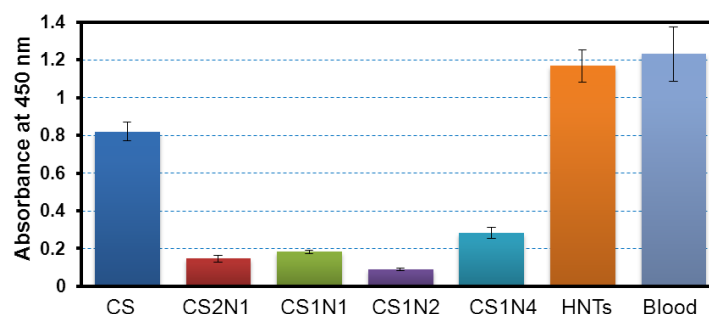
Figure 6 Whole-blood clotting evaluation of the pure chitosan, HNTs and the chitosan-HNTs composite sponges.

Generally, the clotting behavior of wound dressing is related to the chemical composition, morphological features, and 3D microstructure of the materials. Chitosan is a hemostat, which can help in natural blood clotting and blocks nerve endings and hence reducing pain. Chitosan's hemostasis ability can be attributed to the attraction of negatively-charged residues on red blood cell membranes by the protonated amine groups and the adsorption of fibrinogen and plasma proteins. On the other hand, HNTs are porous inorganic nanomaterials with empty lumen structure, resulting

in a high absorption ability to the many types of active compounds. From the clotting experiment

results, we can speculate that HNTs can shorten both the time lag for initial thrombin generation as

well as the time to peak thrombin generation. Therefore, HNTs can accelerate the production of

sufficient amounts of thrombin to support earlier fibrin generation. Due to the interactions between

HNTs and chitosan and the 3D pore structures of the sponges, the composite sponges could trap more

RBCs to enlarge and solidify the growing thrombus, leading to much more rapid and stable clotting

compared with pure chitosan. With respect to the HNTs powder, the low clotting ability can be

attributed to the highly aggregated state of the tubes. The clotting ability of the sponges was further

confirmed by the platelet adhesion experiment via the SEM observation (Figure 7). It can be seen that

the platelets exhibit spread morphology on the sponge surfaces, suggesting the platelets activation

ability of the materials.

(a)   (b)

(c)
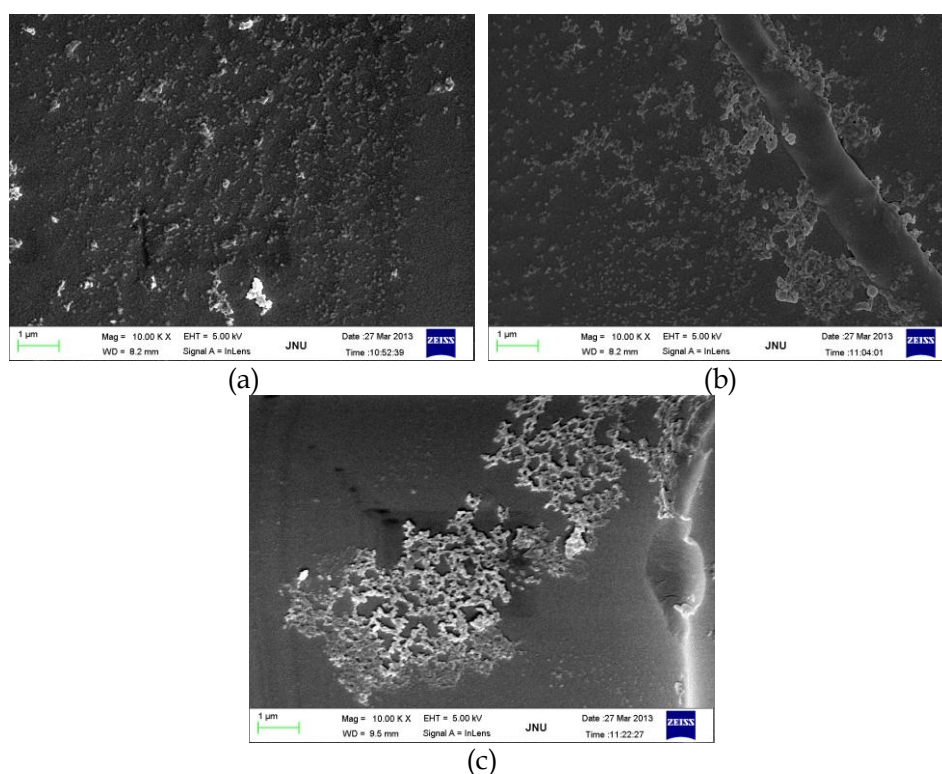
Figure 7 SEM images of platelet activation on pure chitosan (a), CS1N1 (b), and CS1N4 (c) sponges.

Overall, the results of the hemostatic assays show that the CS1N2 sponges is best among the samples

for enhancing hemostasis, since it lead to the fastest blood clotting and platelet adhesion. Since the

swelling ratio in PBS solutions by CS1N2 is comparable with that of chitosan, the enhanced blood

absorption can be attributed to specific attractions of blood proteins and other blood components with

HNTs. The ability of the composite sponges to absorb more blood should assist in stopping high flow

hemorrhage and removing excess exudates at the wound interface.

3.5 Cell Attachment and spread on the chitosan-HNTs composite sponges.

The influence of HNTs on the cytocompatibility of chitosan sponges was assessed using the fibroblasts

and endothelial cells. The morphology, adhesion, and spreading of the cells on pure chitosan and

chitosan-HNTs composite sponges were observed by SEM as a result of the opacity of the composite

films (Figure 8 and Figure 9). The two types of cells can spread on all the samples after 3 day culture.

SEM examination at higher magnification of the cell morphology (Figure 8f) shows cellular extensions

closely interacting with tubular HNTs in the composite sponges even when HNTs loading is as high

as 80 wt.-%, indicating the good cytocompatibility of the inorganic nanotubes. It also can be seen that

the cells on the pure chitosan fail to spread fully. This is not a result from possible toxicity of chitosan,

but can be attributed to the smooth pore wall structures. From the morphology results above, the

pore-walls of the composites are rougher than that of chitosan, therefore, leading to the better

spreading of the cells on them. The cell experiment results demonstrate a promotion effect of HNTs

for the cell attachment and growth due to their high surface roughness of the composites and

biocompatibility of HNTs. In our previous study, the cytocompatibility of HNTs was confirmed using

the osteoblasts and fibroblasts in polyvinyl alcohol (PVA)-HNTs nanocomposites [38]. The

morphological, physicochemical, blood clotting properties and *in vitro* cell attachment and spread

results of the chitosan-HNTs composite sponges imply the possibility of them using as wound

dressing materials. These results stimulated us to evaluate their *in vivo* biological properties using

full-thickness skin wound animal model.

(a)

(b)

(c)

(d)

(e)

(f)
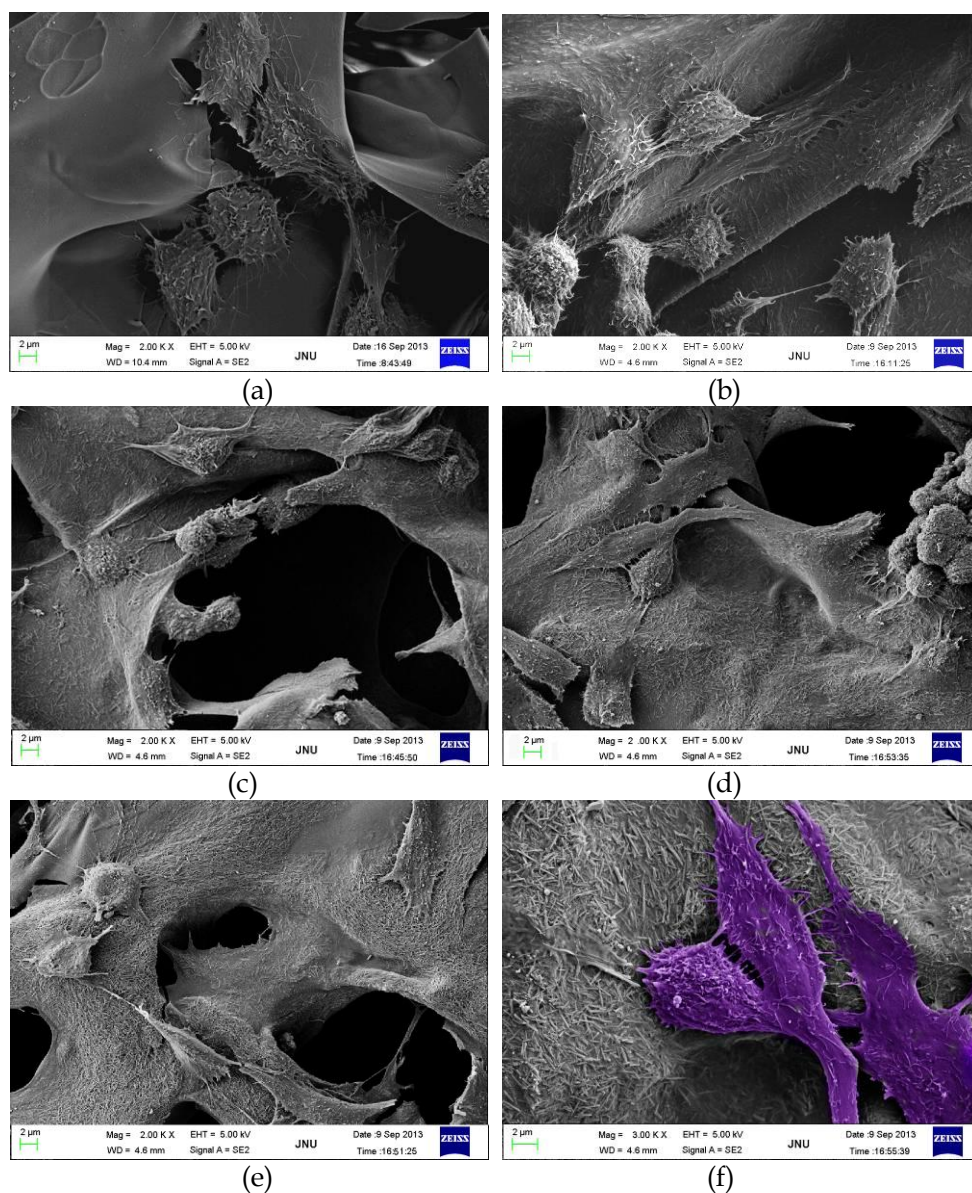
Figure 8 SEM images of fibroblast (NIH3T3) cultured on CS-HNTs nanocomposite scaffolds after 3 day: (a) CS; (b) CS2N1; (c) CS1N1; (d) CS1N2; (e) CS1N4; (f) enlarged image of CS1N2 sample with artificial staining showing the cells.

(a)

(b)
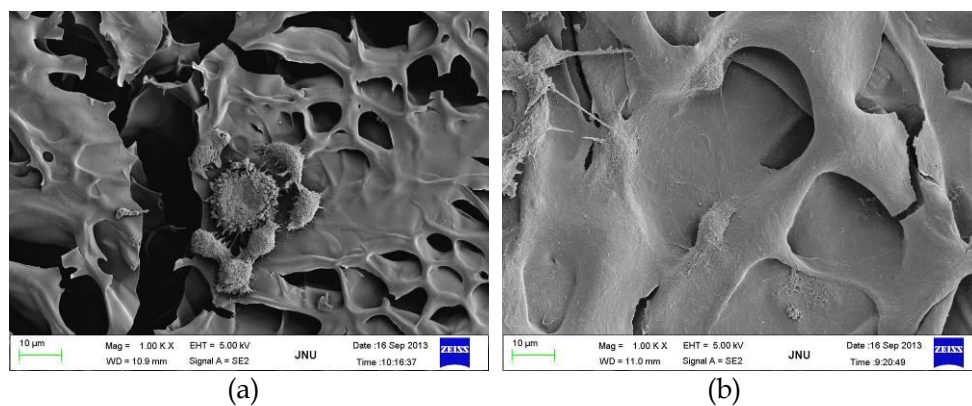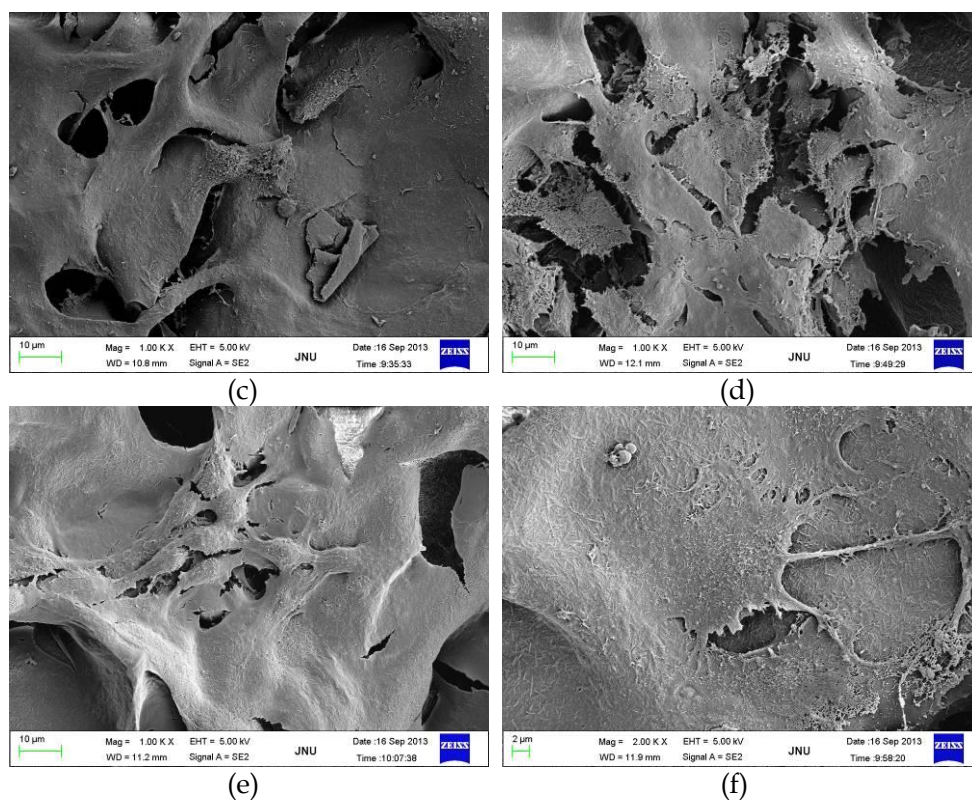
Figure 9 SEM images of vascular endothelial cell cultured on CS-HNTs nanocomposite scaffolds after 3 day: (a) CS; (b) CS2N1; (c) CS1N1; (d) CS1N2; (e) CS1N4; (f) enlarged image of CS1N2 sample.

3.6 *In Vivo* wound healing evaluation of the chitosan-HNTs composite sponges.

In vivo study conducted in SD rats suggested the enhanced wound healing ability of chitosan sponges by HNTs. Figure 10 shows the photographs of the wound healing process after treatment with different materials. At day of surgery, no visible difference in wound appearance is found. Obviously, for all the groups the wound shows granulation tissue formation with the extension of time. Except for the wounds treated by AWD, the wounds in the rats are nearly completely closed after 4 week treatment. The regenerated skin is smooth and similar with normal skin without scar formation after 4 weeks, indicating the good healing ability for the skin tissue by the used materials. With respect to the difference among the groups, the unhealed area of the AWD group is much larger than that of other groups. And the composite sponges have much higher wound healing rate and contraction ability than those of pure chitosan sponges. The extent of wound closure was quantified at different time

points and the results are shown in Figure 11. After one week, the composite sponges show 3.4~21 fold increased closure ratio compared with the pure chitosan. Especially, the CS1N4 sponges show the highest closure ratio of 22%. After two weeks, apart from the AWD and OY groups, the wounds treated with the chitosan-HNTs composite sponges exhibit lineally increased closure ratio with the loading of HNTs. For example, the wound closure of CS1N4 sponges is ~85%, which is 32% higher than that of the pure chitosan sponges. For all groups, the data of closure after three and four weeks have slight differences, suggesting the achievement of wound healing after 3 weeks. The maximum closure at 28 day is 98.0%, which corresponds to the CS1N1 group. The data is sustainably higher than that of pure chitosan groups, which is only 87%. It also should be noted that although the OY can effectively repair the wound, the possibility of secondary damage when removing them limits their applications in skin regeneration.
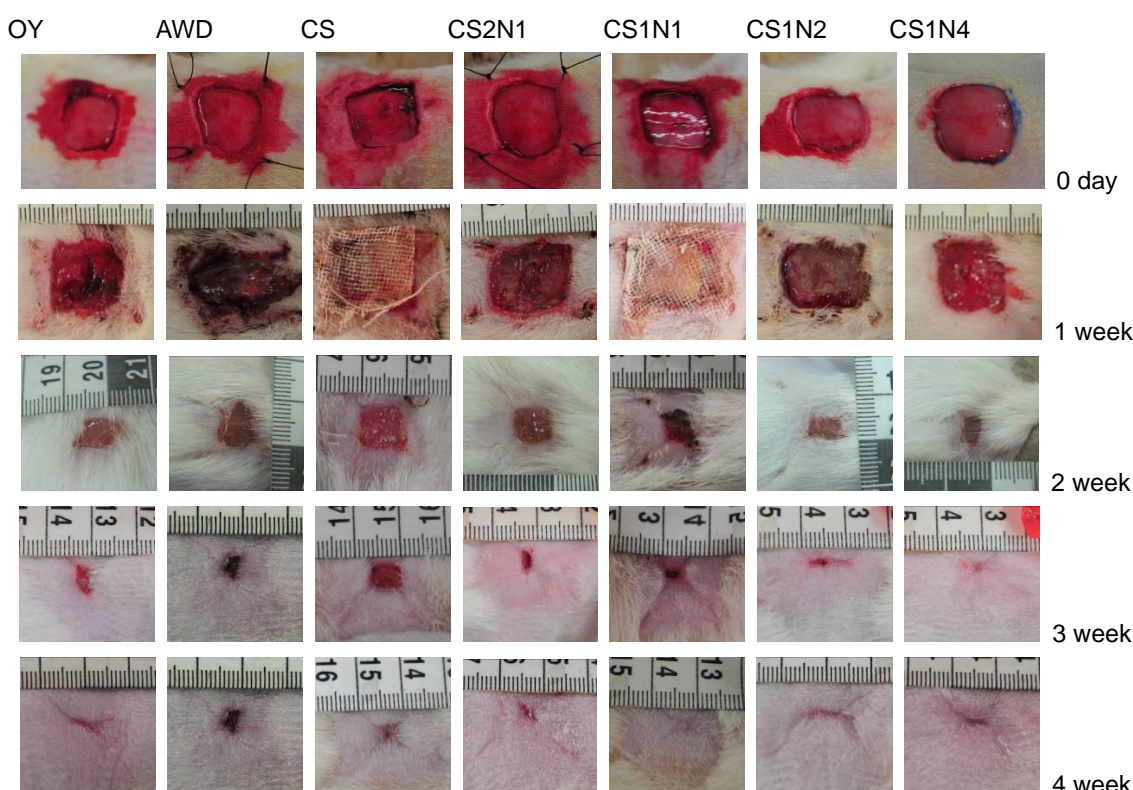
Figure 10 Appearance of wounds treated with oily cotton gauze (OY), adhesive wound dressing (AWD), pure chitosan sponge, and chitosan-HNTs composite sponge.
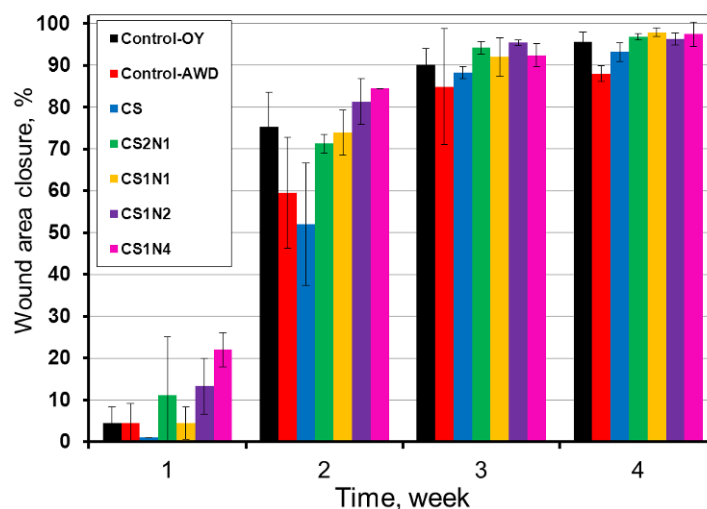
Figure 11 Evaluation of the wound area closure treated by different dressing materials.

From the *in vivo* healing experiment results, we can conclude that the incorporation of HNTs into chitosan can accelerate the wound healing especially at the initial stage. This is attributed to the synergistic effect of chitosan and the HNTs. There are numerous reports on the wound dressing materials based chitosan [25]. The promotion of wound healing and scar prevention is realized by stimulation of the inflammatory cell aggregation and promotion of the cell migration into the wound area by the porous scaffolds [39]. The improvement of wound healing ability of chitosan sponges by HNTs may be attributed to their intrinsic high hemostasis properties and promotion of cell migration into the wound areas. In fact, the raw HNTs were commonly used as wound treatment materials in ancient China, although the mechanism for wound healing was not clear. The related mechanism will be discussed in the following section. Above all, the prepared wound dressing composite sponges have the advantages such as rapid hemostasis, accelerated tissue regeneration, promoted cell attachment, and low cost. Furthermore, HNTs in the composite sponges can be used as a vehicle for biopharmaceuticals, antimicrobials, growth factors, and functional gene to wounds owing to their perfect lumen structures. From a practical point of view, the composite sponges are not dissolve and adhere during the application period to the wound and are easy to remove without ripping the skin.

Therefore, the chitosan-HNTs sponges have promising applications as wound dressing materials in skin or other organ regeneration.

3.7 Histological observation in the wound area.

The final goal for the wound dressing of the skin is restoring the structural and functional properties to the levels of normal tissue, involving re-epithelialization and orchestrated regeneration of all the skin appendages [40]. Figure 12 shows the histological observations for the growth status and structure of epithelial tissue in each group at week 4 after operation. It can be seen that for all the groups the wounds are closed without significant difference with the surrounding normal skin tissue. The areas of epithelialization and granulation tissues including dense fibroblast deposition in the composite sponges groups are found to be larger than those in AWD and OY group. Re-epithelialization on the granulation tissue in open wound can form a barrier between the wound and the environment, which is very important for the wound healing. The epithelialization rate and the deposition of collagen in the dermis are increased by HNTs. The wound treated by the CS1N2 sponge shows the minimum wound area among the groups. Fully differentiated epidermic cells, closely arranged basal cells, and the horny layer and large amounts of hair and sebum are observed in the wound treated by the composite sponges, suggesting a similar epithelial structure with the normal skin. These results suggest HNTs can accelerate the proliferation of neonatal granulation tissue and offered optimum conditions for epithelial cell migration during the wound healing, as well as the production of collagen by fibroblasts.
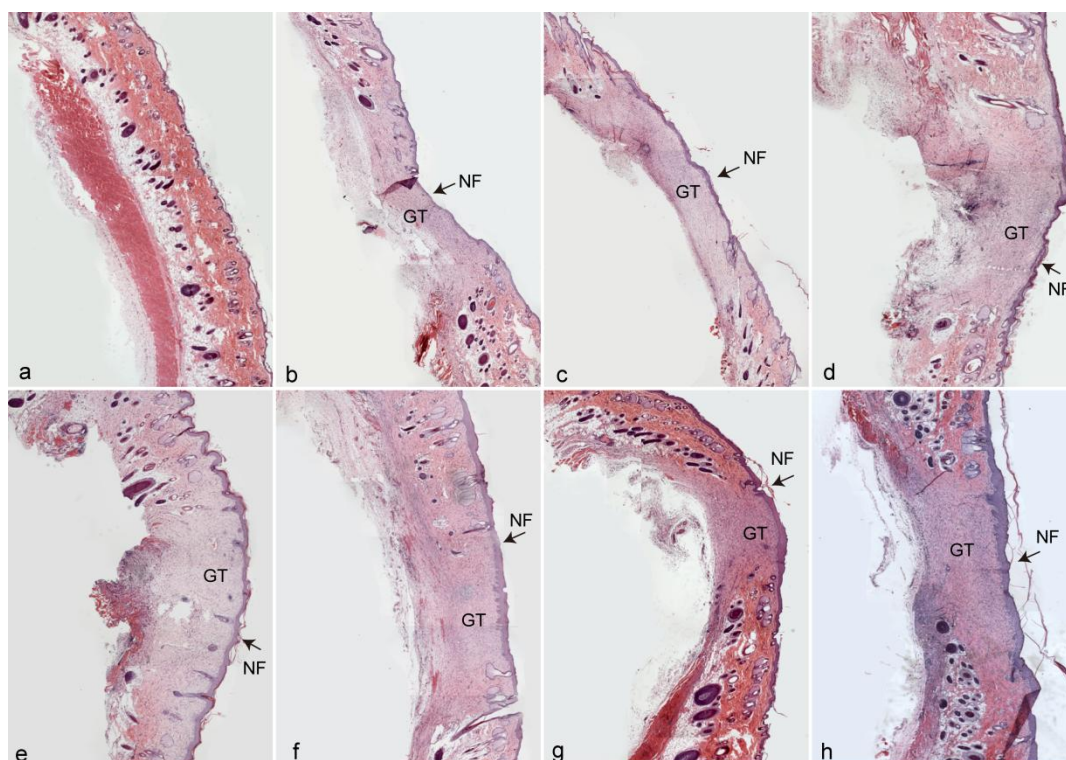
Figure 12 Photomicrographs of hematoxilin and eosin (H&E)-stained normal skin (a), OY treated wounds (b), AWD treated wound (c), pure chitosan sponge treated wound (d), and chitosan-HNTs composite sponge treated wound (e~h, e: CS2N1; f: CS1N1; g:CS1N2; h:CS1N4). The GT represents the granulation tissue and NE represents the neoepidermis.

As shown in the HE staining results above, collagen deposition is observed in all the groups. Additionaly, the amount and the type of collagen fibers are important for the keloids and hypertrophic scar formation. In the present study, Masson and SR staining were used to analysis the collagen deposition and remolding in the regenerated tissues. Figure 13 shows the Masson staining images of the wound for different groups, where the red denotes keratin and muscle fibers, blue or green denotes collagen and bone, light red or pink denote cytoplasm, and dark brown to black denotes cell nuclei. The collagen fibers are fine and matured in the wound treated by the composite sponges, and their arrangement is similar to that of native skins. Figure 14 shows the polarizing microscope images of collagen fibers by SR staining, where the yellow/red color denotes collagen type I, red/white denotes collagen II, green denotes collagen type III and light yellow denotes collagen type IV. It can be seen that the type I collagen is the main component for the native skin. At

26

week 4 after operation, the regenerated tissue in all the groups consists chiefly of collagen type I, with

a small amount of other type collagen interspersed, which is close to the profile of native skin. This

also suggests the good healing ability of the composite sponges as well as the chitosan sponges.
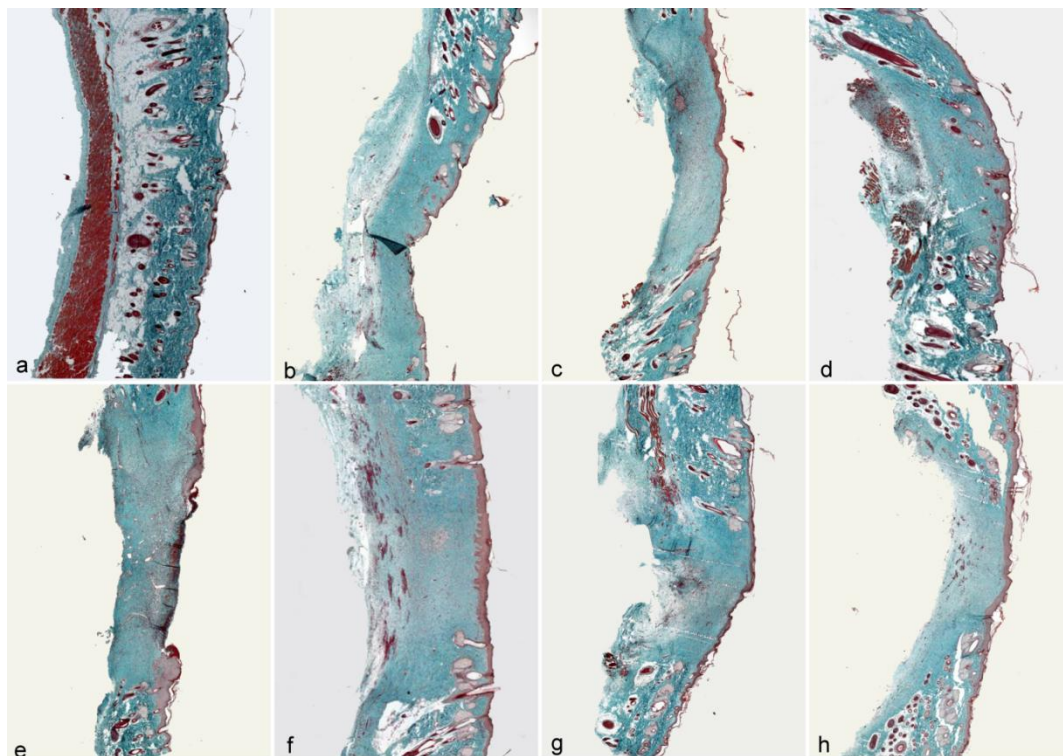
Figure 13 Photomicrographs of Masson-stained normal skin (a), OY treated wounds (b), AWD treated wound (c), pure chitosan sponge treated wound (d), and chitosan-HNTs composite sponge treated wound (e~h, e: CS2N1; f: CS1N1; g:CS1N2; h:CS1N4).
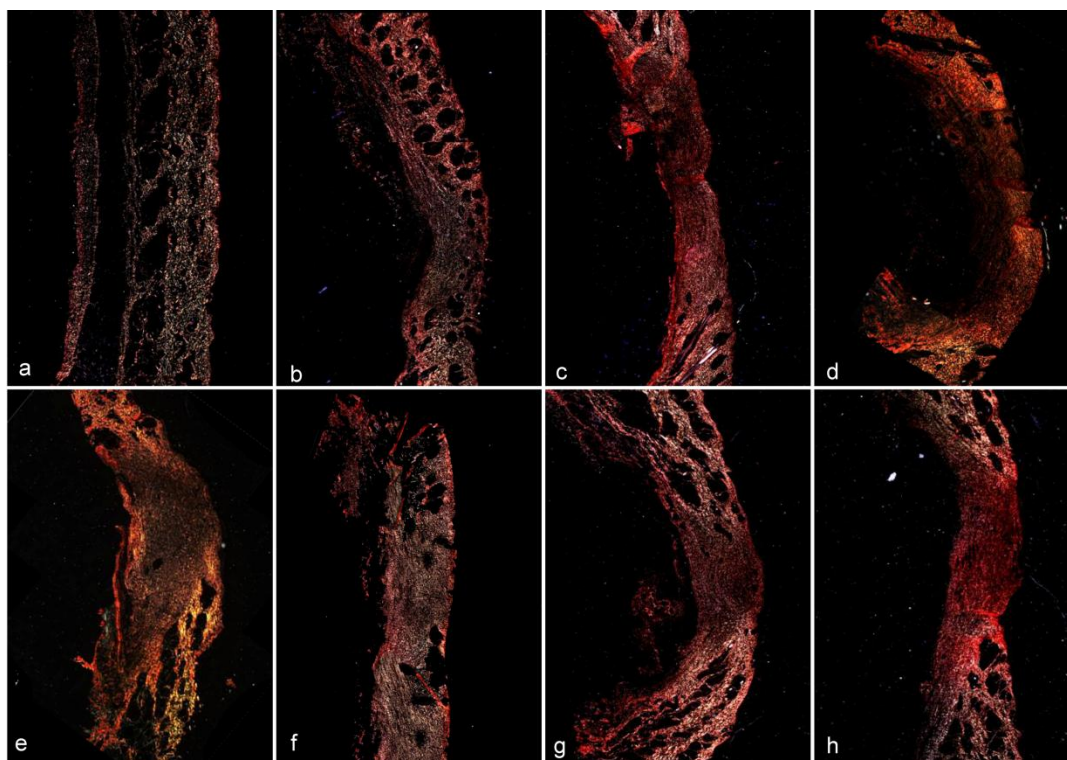
Figure 14 Polarimicroscope images of SR-stained normal skin (a), OY treated wounds (b), AWD treated wound (c), pure chitosan sponge treated wound (d), and chitosan-HNTs composite sponge treated wound (e~h, e: CS2N1; f: CS1N1; g:CS1N2; h:CS1N4).

Wound healing is a complex process which consists of a series of coordinated overlapping biological events, involving acute and chronic inflammations, cell division, and extracellular matrix (ECM) synthesis. From the histological studies by the different staining, expect the AWD, all the dressing materials exhibit good healing ability for the wound injury. Especially, the chitosan-HNTs composite sponges show improved wound healing ability. The mechanisms involved in the beneficial healing activity should be attributed to the unique characters of HNTs. HNTs in the composite markedly increase the nano-roughness of the pore-wall for the sponges, which, in turn, could (i) favor the trapping of factors detrimental to the repair process when present in excess (proteases, reactive oxygen species, etc.), (ii) stimulate the progressive release of active fragments that are reported to recruit and activate leukocytes and mesenchymal cells, and (iii) increase the surface available for protein coating and cell adhesion. Also the enhancement of the mechanical property of the chitosan sponges by HNTs strongly regulates the phenotype and the differentiation process of the cells. In total,

the highly porous structure and high mechanical properties of the chitosan-HNTs composite sponges

allow the gaseous and fluid exchanges, stop bleeding and absorb excess exudates, facilitate the cells

attachment and spread, and promote the healing of the wounds, indicating one of the most suitable

wound dressing materials. And among the sample, the CS1N2 sponges with 33 wt.-% chitosan and 66

wt.-% HNTs exhibit overall performance results. It shows 89.0% increase in the clotting ability and

12%, 29.3%, 7.1% and 3.1% increase in the wound closure ratio after 1, 2, 3, 4 weeks respectively

compared with pure chitosan sponges.

4. Conclusions

The chitosan-HNTs composite sponges with different HNTs loadings are prepared by lyophilization.

The addition of HNTs slightly affects the pore structure of the chitosan sponge even with 80 wt.-%. A

slightly decreasing trend in porosity and weight loss in PBS of the composite sponges is obtained with

incorporation of the HNTs. The swelling ratios of the pure chitosan and chitosan-HNTs sponges in

PBS solutions are comparable. HNTs can enhance the elastic modulus, compressive strength, and

toughness of the chitosan sponges simultaneously. The fibroblasts and endothelial cells can spread

well in the composite sponges, indicating their good cytocompatibility. The composite sponges show

enhanced blood clotting and platelet activation ability. The composite sponges with 67% HNTs shows

89.0% increase in the clotting ability compared with pure chitosan. *In vivo* wound healing evaluation

confirms the enhanced healing ability of the chitosan sponges by HNTs. The composite sponges show

3.4~21 fold increased wound closure ratio compared with that of pure chitosan after one week. The

addition of HNTs helps for faster re-epithelialization and collagen deposition. All these are attributed

to the unique characteristics of HNTs and the synergistic effect of chitosan and the HNTs. Overall

results demonstrate that these advanced chitosan-HNTs composite sponges have many potential

applications for burn, chronic, and diabetic wound infections.

Reference:

[1]   M. Ishihara, K. Nakanishi, K. Ono, M. Sato, M. Kikuchi, Y. Saito, H. Yura, T. Matsui, H. Hattori, M. Uenoyama, A. Kurita, *Biomaterials* **2002**, *23*, 833.

[2]   B. Balakrishnan, M. Mohanty, P. R. Umashankar, A. Jayakrishnan, *Biomaterials* **2005**, *26*, 6335.

[3]   M. S. Khil, D. I. Cha, H. Y. Kim, I. S. Kim, N. Bhattarai, *J. Biomed. Mater. Res., Part B* **2003**, *67B*, 675.

[4]   F. L. Mi, S. S. Shyu, Y. B. Wu, S. T. Lee, J. Y. Shyong, R. N. Huang, *Biomaterials* **2001**, *22*, 165.

[5]   K. Ulubayram, A. N. Cakar, P. Korkusuz, C. Ertan, N. Hasirci, *Biomaterials* **2001**, *22*, 1345.

[6]   L. Huang, K. Nagapudi, R. P. Apkarian, E. L. Chaikof, *J. Biomater. Sci., Polym. Ed.* **2001**, *12*, 979.

[7]   S. Agarwal, J. H. Wendorff, A. Greiner, *Polymer* **2008**, *49*, 5603.

[8]   J. S. Boateng, K. H. Matthews, H. N. E. Stevens, G. M. Eccleston, *J. Pharm. Sci.* **2008**, *97*, 2892.

[9]   M. Kumar, *React. Funct. Polym.* **2000**, *46*, 1.

[10] E. Khor, L. Y. Lim, *Biomaterials* **2003**, *24*, 2339.

[11] H. Ueno, H. Yamada, I. Tanaka, N. Kaba, M. Matsuura, M. Okumura, T. Kadosawa, T. Fujinaga, *Biomaterials* **1999**, *20*, 1407.

[12] F. Bergaya, G. Lagaly, *Handbook of Clay Science, 2nd Edition*, Elsevier, Oxford OX5 1GB, UK **2013**.

[13] D. Depan, A. P. Kumar, R. P. Singh, *Acta Biomaterialia* **2009**, *5*, 93.

[14] Y. Lvov, E. Abdullayev, *Prog. Polym. Sci.* **2013**, *38*, 1690.

[15] P. Luo, Y. F. Zhao, B. Zhang, J. D. Liu, Y. Yang, J. F. Liu, *Water Res.* **2010**, *44*, 1489.

[16] R. R. Price, B. P. Gaber, Y. Lvov, *J. Microencapsulation* **2001**, *18*, 713.

[17] M. Liu, C. Wu, Y. Jiao, S. Xiong, C. Zhou, *J. Mater. Chem. B* **2013**, *1*, 2078.

[18] R. Qi, R. Guo, M. Shen, X. Cao, L. Zhang, J. Xu, J. Yu, X. Shi, *J. Mater. Chem.* **2010**, *20*, 10622.

[19] M. Sirousazar, M. Kokabi, Z. M. Hassan, *J. Biomater. Sci., Polym. Ed.* **2011**, *22*, 1023.

[20] S. T. Oh, W. R. Kim, S. H. Kim, Y. C. Chung, J. S. Park, *Fibers Polym.* **2011**, *12*, 159.

[21] R. Huey, D. Lo, D. J. Burns,   *WO2008054566 A1*, **2008**.

[22] Z. Xie, C. B. Paras, H. Weng, P. Punnakitikashem, L.-C. Su, K. Vu, L. Tang, J. Yang, K. T. Nguyen, *Acta Biomaterialia* **2013**, *9*, 9351.

[23] M. Dai, X. Zheng, X. Xu, X. Kong, X. Li, G. Guo, F. Luo, X. Zhao, Y. Q. Wei, Z. Qian, *Journal of Biomedicine and Biotechnology* **2009**, *2009*, 8.

[24] S.-Y. Ong, J. Wu, S. M. Moochhala, M.-H. Tan, J. Lu, *Biomaterials* **2008**, *29*, 4323.

[25] R. Jayakumar, M. Prabaharan, P. T. Sudheesh Kumar, S. V. Nair, H. Tamura, *Biotechnology Advances* **2011**, *29*, 322.

[26] P. T. Sudheesh Kumar, V.-K. Lakshmanan, T. V. Anilkumar, C. Ramya, P. Reshmi, A. G. Unnikrishnan, S. V. Nair, R. Jayakumar, *ACS Applied Materials & Interfaces* **2012**, *4*, 2618.

[27] M. Liu, Y. Zhang, C. Wu, S. Xiong, C. Zhou, *Int. J. Biol. Macromol.* **2012**, *51*, 566.

[28] Y. Xu, X. Ren, M. A. Hanna, *J. Appl. Polym. Sci.* **2006**, *99*, 1684.

[29] X. Cheng, Y. Li, Y. Zuo, L. Zhang, J. Li, H. Wang, *Materials Science and Engineering: C* **2009**, *29*, 29.

[30] D. O. Costa, P. D. H. Prowse, T. Chrones, S. M. Sims, D. W. Hamilton, A. S. Rizkalla, S. J. Dixon, *Biomaterials* **2013**, *34*, 7215.

[31] A. Singer, M. Zarei, F. M. Lange, K. Stahr, *Geoderma* **2004**, *123*, 279.

[32] M. T. Qurashi, H. S. Blair, S. J. Allen, *J. Appl. Polym. Sci.* **1992**, *46*, 255.

[33] L. J. Sweetman, S. E. Moulton, G. G. Wallace, *Journal of Materials Chemistry* **2008**, *18*, 5417.

[34] R. Jayakumar, R. Ramachandran, V. V. Divyarani, K. P. Chennazhi, H. Tamura, S. V. Nair, *International Journal of Biological Macromolecules* **2011**, *48*, 336.

[35] A. W. Seifert, S. G. Kiama, M. G. Seifert, J. R. Goheen, T. M. Palmer, M. Maden, *Nature* **2012**, *489*, 561.

[36] S. K. P. T, V.-K. Lakshmanan, M. Raj, R. Biswas, T. Hiroshi, S. Nair, R. Jayakumar, *Pharm. Res.* **2013**, *30*, 523.

[37] B. S. Anisha, D. Sankar, A. Mohandas, K. P. Chennazhi, S. V. Nair, R. Jayakumar, *Carbohydr. Polym.* **2013**, *92*, 1470.

[38] W. Y. Zhou, B. C. Guo, M. X. Liu, R. J. Liao, A. B. M. Rabie, D. M. Jia, *J. Biomed. Mater. Res., Part A* **2009**, *93A*, 1574.

[39] T. H. Dai, M. Tanaka, Y. Y. Huang, M. R. Hamblin, *Expert Review of Anti-Infective Therapy* **2011**, *9*, 857.

[40] Y. Yang, T. Xia, F. Chen, W. Wei, C. Liu, S. He, X. Li, *Mol. Pharm.* **2012**, *9*, 48.

32